



ELSEVIER

Available online at www.sciencedirect.com

SCIENCE @ DIRECT®

Earth and Planetary Science Letters 228 (2004) 355–367

EPSL

www.elsevier.com/locate/epsl

Signature of magnetic enhancement in a loessic soil in Nebraska, United States of America

Christoph E. Geiss^{a,*}, C. William Zanner^b, Subir K. Banerjee^c, Minott Joanna^d

^aDepartment of Physics, Trinity College, McCook Hall 105, 300 Summit Street, Hartford, CT 06106, United States

^bSchool of Natural Sciences, University of Nebraska, 133 Keim Hall, Lincoln, NE 68583-0915, United States

^cUniversity of Minnesota, Newton Horace Winchell School of Earth Sciences, Pillsbury Drive 310, Minneapolis, MN 55455, United States

^dMt. Holyoke College, Mount Holyoke College, South Hadley, MA 01075-6419, United States

Received 3 May 2004; received in revised form 7 October 2004; accepted 12 October 2004

Available online 21 November 2004

Editor: V. Courtillot

Abstract

Our study of a loessic soil profile from east-central Nebraska shows that the A horizons of the modern soil are characterized by higher concentrations of fine-grained ($<0.1 \mu\text{m}$) magnetic minerals. This pedogenic magnetic component leads to higher values of concentration-dependent parameters, such as magnetic susceptibility (χ), isothermal remanent magnetization (IRM) and anhysteretic remanent magnetization (ARM), combined with increases in frequency-dependent susceptibility (χ_{fd}) and ARM/IRM ratios. Hysteresis properties are relatively insensitive towards the presence of this pedogenic magnetic component.

The magnetic properties of the soil profile are dominated by ferrimagnetic magnetite or maghemite. Analyses of “soft” IRM (sIRM) and “hard” IRM (hIRM), however, do show that approximately 80–90% of the remanence carrying magnetic component exists in the form of hematite or goethite and that the magnetically enhanced horizons are enriched in both ferri- and antiferromagnetic minerals.

The pedogenic magnetic component is most likely caused by the conversion of paramagnetic, iron-bearing minerals to ferri- and antiferromagnetic minerals. Soil compaction, lessivage or decalcification cannot explain the observed magnetic soil properties. Magnetic analyses of loess-paleosol sequences from the midwestern United States may yield valuable information about regional variability of paleoclimate. Based on the fine-grained nature of the pedogenic magnetic component, we expect grain-size-dependent proxies (ARM, ARM/IRM, χ_{fd}) to yield better paleoclimatic information than low-field magnetic susceptibility used in previous analyses.

© 2004 Elsevier B.V. All rights reserved.

Keywords: environmental magnetism; loess; soil; Holocene; Nebraska; climate reconstruction

* Corresponding author. Tel.: +1 860 297 4191; fax: +1 860 987 6239.

E-mail addresses: christoph.geiss@trincoll.edu (C.E. Geiss), czanner@unlnotes.unl.edu (C.W. Zanner), banerjee@umn.edu (S.K. Banerjee), jminott@hotmail.com (M. Joanna).

1. Introduction

Over the last decades, rock-magnetic analyses of loess-paleosol sequences have provided valuable tools for the reconstruction of paleoclimatic change in mid-continental regions, where other recorders of climate are rare or absent. Numerous studies of the Chinese loess plateau show that modern and buried soils are characterized by higher concentrations of magnetic minerals in the A and B horizons. The degree of this magnetic enhancement is often quantified by changes in magnetic susceptibility between the enhanced horizons and the pedogenetically unaltered parent material (e.g., [1]). Several studies have shown a good correlation between the magnitude of magnetic enhancement in modern soils and present climatic conditions, especially rainfall (e.g., [2–4]), even though the processes that lead to the observed magnetic signal remain under discussion [5].

In situ formation of (ultra)fine-grained ($<0.1 \mu\text{m}$) ferrimagnetic minerals through a variety of processes is likely to explain the magnetic enhancement found in many loess-paleosol sequences in China, Europe and the North America. Potential pathways include the effects of repeated fires [6–8], changes in redox conditions due to plant decomposition [6,9] or repeated wetting and drying cycles in otherwise well-drained soils [10], and the effects of bacterial

activity [11]. Soil compaction and loss of weakly magnetic minerals through decalcification [12] or leaching [13] have also been suggested as potential pathways of magnetic enhancement. Paleosols in Alaska and Siberia, however, are often characterized by low concentrations of magnetic minerals, compared to their loessic parent material. Such low concentrations might be due to the loss of iron oxide minerals during periods of gleying [14] or changes in wind vigor [15,16], which can result in changed sediment compositions. Singer et al. [17], Maher [18] and Tang et al. [5] provide additional information on the pathways of magnetic enhancement in soils and the relationship between soil magnetic properties and climate.

While the influence of climate on soil magnetic properties is well established, it is less clear over which time periods the magnetic signature of soils continues to evolve. Based on evidence from modern or recently disturbed soils [19], as well as loess-paleosol sequences from the western edge of the Chinese loess plateau [20], Maher et al. argue that the magnetic enhancement signature is acquired rapidly within a few centuries. Analyses of a chronosequence from California by Singer et al. [21] and a loess-paleosol sequence from Jiaodao, China by Vidic et al. [22], however, suggest that the magnetic signal of soils continues to evolve, probably over several 100,000 years.

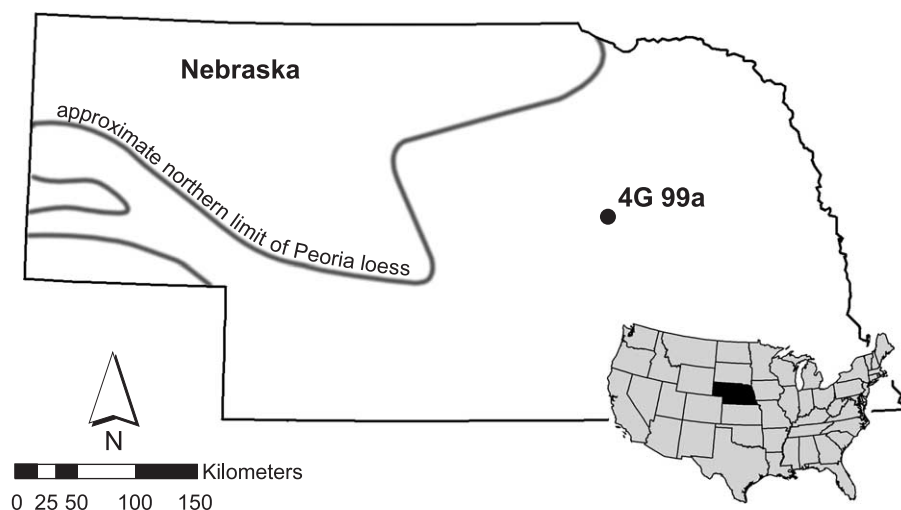


Fig. 1. Location of soil site 4G-99a in east-central Nebraska. Map insert shows location within continental United States. The approximate extent of Pleistocene Peoria loess is indicated by a light gray line (modified after [28]).

Unfortunately, successful application of magnetic proxies to the Chinese loess for paleoclimate reconstruction is not automatically extended to other loess regions. In Europe and Russia, many loessic modern and buried soils [4,18] show magnetically enhanced soil horizons, but some paleosols that formed during marine isotope stage 5 show a depletion of pedogenic ferrimagnetic magnetic minerals, possibly due to intense weathering [23,24]. As mentioned above, some paleosols in Alaska and Siberia contain low abundances of ferrimagnetic minerals, though the modern soils are still enhanced in magnetic minerals [25]. It is therefore necessary to establish the nature of the soil-magnetic signal for a given region before any attempts of paleoclimatic reconstructions can be made.

Relatively few studies [26,27] are concerned with the magnetic properties of loess-paleosol sequences in the midwestern United States. The central Great Plains is an ecologically and agriculturally important semi-

arid region. Twenty-five percent of the world's total production of wheat, corn, barley, oats, rye and sorghum are grown here, at the threshold limits of needed rainfall, and dependence on artificial irrigation from rivers and aquifers is high. Despite the region's dependence on natural rainfall, little is known about the variability of past climatic conditions, which is mostly due to the absence of good recorders of paleoclimate, such as lake basins or cave deposits. A magnetic analysis of soils and paleosols offers the opportunity to reconstruct paleoclimatic conditions for certain time slices. However, the absence of an universally applicable link between pedogenic magnetic enhancement and climate makes it necessary to carefully investigate the magnetic signature of modern soils before any climate reconstruction can be attempted. In this study, we use a magnetic multi-proxy approach to carefully characterize the magnetic properties of a modern loessic soil from east-central Nebraska, to constrain possible pathways of magnetic enhancement, and to

Table 1
Soil description for site 4G-99a

Depth	Horizon	Boundary	Color	Texture	Structure	Effervescence	Other
0–20	Ap	clear	very dark gray (10YR 3/1)	heavy silt loam	weak fine to medium granular	none	
20–33	A	clear	very dark gray (7.5YR 3/1)	light silty clay loam	fine granular	none	
33–44	Bt1	clear	brown (10YR 4/3)	silty clay loam	moderate very fine and fine subangular blocky	none	many thin continuous clay coatings (10YR 3/1) on ped faces
44–69	Bt2	gradual	light olive brown (2.5Y 5/3)	silty clay loam	moderate fine subangular blocky	none	many thick, slightly patchy (2.5Y 4/2) clay coatings on ped faces
69–91	Bt3	clear	light olive brown (2.5Y 5/3)	heavy silt loam	moderate medium subangular blocky	none	many thin patchy (2.5Y 4/2) clay coatings on ped faces
91–120	BC	clear	light olive brown (2.5Y 5/3)	silt loam	weak medium to coarse subangular blocky	none	very few fine (2.5Y 6/1) Fe depletions, very few fine 10YR 5/6 Fe concentrations
120–135	Ck1	gradual	light olive brown (2.5Y 5/3)	silt loam	weak medium subangular blocky	weak	common fine and medium CaCO ₃ concentrations
135–200	Ck2	gradual	light olive brown (2.5Y 5/3)	silt loam, high in very fine sand	weak coarse subangular blocky	none in matrix	common fine CaCO ₃ concentrations, less than in Ck1, faint sedimentary laminations (1–5 mm thick)
200–235	C		light olive brown (2.5Y 5/3)	silt loam, high in very fine sand	massive	none	few fine 10YR 5/6 Fe concentrations

Description kindly provided by Joe Mason, University of Wisconsin.

suggest magnetic parameters that might yield reliable proxies for paleoclimate reconstructions.

2. Site description

The site was sampled with a 7.6-cm (3-in.)-diameter hydraulic soil probe and described by Dr. J. Mason in 1999. The dried cores were subsampled in 2000, and samples were packed tightly into weakly diamagnetic plastic cubes for magnetic analyses.

Core 4G-99a was collected from a broad (~130 m) ridge top in Boone County, Nebraska (41.5191°N, 98.2127°W; Fig. 1). Uplands in this region of Nebraska are blanketed by approximately 1–20 m of Wisconsin Peoria loess underlain by Illinoian Loveland loess. Some areas have been influenced by minor Holocene loess deposition. Presettlement vegetation was prairie. For the period between 1961 and 1990, mean precipitation was 710 mm/year and mean annual temperature was 8.7°C (minimum=1.5°C, maximum=15.9°C) [29]. The area around the core is mapped as Hord silt loam, and classified at the time of the survey as a fine-silty, mixed, mesic Pachic Haplustoll [30].

The profile horization is Ap-A-Bt1-Bt2-Bt3-BC-Ck1-Ck2-C (see also Fig. 4). Textures are silt loam in the Ap and Bt3-BC-Ck1-Ck2-C horizons with A, Bt1 and Bt2 horizons being silty clay loam. Ap and A horizons have granular structure and very dark gray (10YR3/1) colors. The C horizon is massive; remaining horizons have subangular blocky structure that increases in size with depth. Bt horizons are light olive brown (2.5Y5/3) with clay coatings. There are very few <2 mm distinct (2.5 Y6/1) and prominent (10YR5/6) mottles in the BC (90–120 cm) and C (>200 cm) horizons, which are light olive brown (2.5Y5/3). The Ck horizons are light olive brown (2.5 Y5/3) and have <5 mm carbonate masses. A complete description of site 4G-99a is given in Table 1.

3. Methods

We characterized the magnetic mineralogy and abundance of ultrafine (<0.01 μm) (super)paramagnetic particles through thermal demagnetization of isothermal remanent magnetization (IRM), acquired

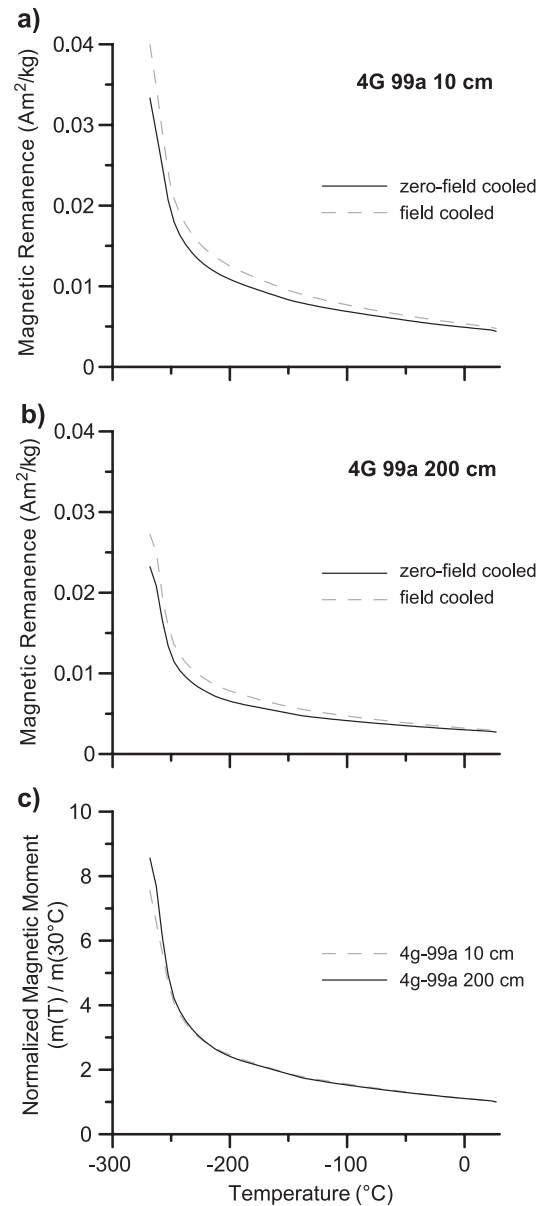


Fig. 2. (a,b) Thermal demagnetization curves of low-temperature IRM, acquired at -268.15°C in 2.5 T after cooling the samples from room temperature in a magnetic field of 2.5 T (dashed gray) and after cooling in zero field (solid black). Shown are the results from 10 and 200 cm depth. The drop in magnetic remanence at low temperatures is due to the thermal demagnetization of (super)paramagnetic minerals. (b) Zero-field cooled demagnetization curves, normalized by the magnetic moment at room temperature after demagnetization. Both curves are rather similar and show a marked drop in magnetic moment at low temperatures due to thermal unblocking of (super)paramagnetic particles. The Verwey transition, diagnostic of magnetite, is barely visible near -155°C .

at 5 K (-268.15°C) for several samples [31]. These analyses were performed on a Quantum Design Magnetic Measurement System (MPMS 5s). Curie temperature determinations aided in the characterization of the magnetic mineralogy [32] and were performed in an inert gas atmosphere on a AGICO Kappabridge KLY-2 with modified furnace apparatus.

To estimate the concentrations of remanence carrying magnetic minerals, we acquired IRM at DC fields of 100 and 1300 mT and at backfields of -300 and -600 mT (Table 2). We distinguished between high- and low-coercivity minerals by calculating “hard” IRM ($\text{hIRM}=0.5 (\text{IRM}_{1300 \text{ mT}}+\text{IRM}_{-\text{backfield}})$) and “soft” IRM ($\text{sIRM}=0.5 (\text{IRM}_{1300 \text{ mT}}-\text{IRM}_{-\text{backfield}})$) [33,34]. Measurements for hIRM and sIRM were repeated five times per sample and the resulting standard deviation is shown in Fig. 4g. Anhysteretic remanent magnetization (ARM) was acquired in a peak AF-field of 100 mT and a bias field of $50 \mu\text{T}$, using a D-Tech 100 mT 2000 AF demagnetizer. The ratio of $\text{ARM}/\text{IRM}_{100 \text{ mT}}$ was used as a proxy for the relative

abundance of single domain (SD) magnetic particles [35,36]. The relative abundance of low- and high-coercivity minerals was estimated from S -ratios ($S_{300}=-\text{IRM}_{-300 \text{ mT}}/\text{IRM}_{1300 \text{ mT}}$) [37]. All remanence parameters were measured in a cryogenic magnetometer (2G, Model 760-R) with a nominal sensitivity of $2 \times 10^{-11} \text{ A m}^2$. Low-field susceptibility (χ) was measured using a Kappabridge KLY-2 susceptibility meter with a nominal sensitivity of $4 \times 10^{-8} \text{ SI}$. Frequency-dependent susceptibility (χ_{fd}), a proxy for the presence of superparamagnetic (SP) particles [38], was measured at 20 frequencies between 40 and 4000 Hz. Frequency values for 400 and 4000 Hz were obtained from a best fit through the entire data set to calculate $\chi_{\text{fd}}=(\chi_{400 \text{ Hz}}-\chi_{4000 \text{ Hz}})/\chi_{400 \text{ Hz}}$. The errors associated with the measurement and shown in Fig. 4c were calculated from the error of the best fit line and the resulting error for $\chi_{400 \text{ Hz}}$ and $\chi_{4000 \text{ Hz}}$. Hysteresis loops were measured for selected samples in a maximum field of 1300 mT using a vibrating sample magnetometer (Princeton Applied Research, modified by the Institute for Rock

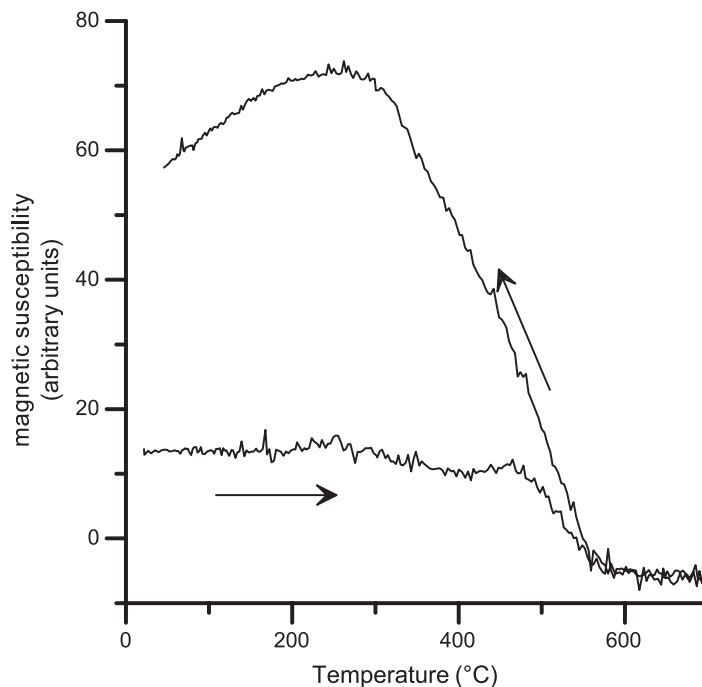


Fig. 3. Curie temperature (T_C) measurement for a sample from 20 cm depth. A Curie temperature of 570°C suggests a ferrimagnetic component close to magnetite as the principal magnetic mineral. The increase in susceptibility upon heating is likely due to the reduction of weakly magnetic antiferromagnetic minerals, such as goethite or hematite, to magnetite.

Table 2
Magnetic properties for samples from site 4G-99a

Depth (cm)	χ_{if} ($\text{m}^3/\text{kg} \times 10^{-6}$)	ARM ($\text{mA m}^2/\text{kg}$)	IRM _{100 mT} ($\text{mA m}^2/\text{kg}$)	ARM/IRM _{100 mT} (%)	χ_{fd} (%)	M_s ($\text{mA m}^2/\text{kg}$)	M_{rs} ($\text{mA m}^2/\text{kg}$)	H_c (mT)
0–5	0.81	0.18	6.10	2.97	4.0±1.2	58.70	6.01	8.4
5–10	0.84	0.17	5.93	2.88	4.0±1.2	61.90	6.53	
10–15	0.83	0.19	4.99	3.72	4.4±1.2	55.20	5.95	8.21
15–20	0.76	0.17	4.78	3.61	4.0±1.8	52.00	5.40	8.51
20–25	0.76	0.16	5.20	3.13	3.8±1.5	48.90	5.30	8.72
25–30	0.75	0.16	5.21	3.03	3.4±1.2	29.00	2.92	8.26
30–35	0.56	0.11	3.91	2.90	3.2±1.5	41.80	4.22	8.36
35–40	0.55	0.11	3.86	2.85	2.1±2.1	37.70	3.84	8.32
40–45	0.50	0.09	3.54	2.54		34.70	3.66	8.61
45–50	0.54	0.09	3.86	2.42	1.2±1.9	32.20	3.39	8.61
50–55	0.50	0.08	3.65	2.29		33.00	3.40	8.66
55–60	0.46	0.07	3.35	2.07	1.0±1.8	34.70	3.59	8.69
60–65	0.46	0.07	3.46	2.02		31.90	3.32	8.77
65–70	0.48	0.07	3.64	1.93		32.10	3.62	7.82
70–75	0.43	0.06	3.23	1.95		32.10	3.47	8.74
75–80	0.45	0.06	3.47	1.77	0.5±1.9	33.50	3.48	8.81
80–85	0.46	0.07	3.51	1.85		33.00	3.51	8.78
85–90	0.50	0.07	3.96	1.71		35.70	3.68	8.74
90–95	0.48	0.06	3.50	1.86		36.80	3.86	8.66
95–100	0.43	0.06	3.52	1.62	1.1±1.3	34.50	3.66	8.69
100–105	0.48	0.06	3.33	1.94				
105–110	0.46	0.06	3.73	1.56				
115–120	0.47	0.06	3.77	1.60				
120–125	0.47	0.06	3.81	1.59				
125–130	0.39	0.05	3.19	1.60				
135–140	0.46	0.06	3.71	1.63				
140–145	0.54	0.07	4.11	1.76				
145–150	0.48	0.07	4.08	1.64				
150–155	0.43	0.06	3.35	1.65				
155–160	0.47	0.06	3.61	1.72	0.4±1.9			
165–170	0.48	0.06	3.76	1.61				
170–175	0.43	0.06	3.45	1.60				
175–180	0.48	0.06	3.72	1.65				
180–185	0.42	0.06	3.29	1.72				
185–190	0.44	0.06	3.35	1.68				
190–195	0.42	0.06	3.31	1.69				
200–205	0.53	0.07	4.15	1.58				
205–210	0.49	0.06	3.78	1.61				

Magnetism) to estimate bulk magnetic particle size in a plot of saturation remanent magnetization/saturation magnetization vs. coercivity of remanence/coercive force (J_{rs}/J_s vs. H_{cr}/H_c) [39,40], and to correct for the χ_{hf} presence of para- or diamagnetic minerals using the high-field slope χ_{hf} of the hysteresis loop [32]. Concentrations of major and trace elements were measured for three magnetically enhanced horizons and two samples from the unaltered parent material using an Inductively

Coupled Plasma Mass Spectrometer (ICP-MS, Perkin-Elmer/Sciex Elan 5000).

4. Results

Thermal demagnetization curves of low-temperature IRM show a distinct drop at temperatures below -250°C for all samples (Fig. 2), which indicates that para- and superparamagnetic minerals are abundant

H_{cr} (mT)	χ_{hf} (m ³ /kg)	J_{rs}/J_s	H_{cr}/H_c	S_{300}	hIRM _{300 mT} (mA m ² /kg)	hIRM _{600 mT} (mA m ² /kg)	sIRM _{300 mT} (mA m ² /kg)
25.85	3.76E-08	0.102	3.077	0.927±0.003	0.27±0.01	0.13±0.03	7.30±0.02
	3.90E-08	0.105		0.934±0.003	0.27±0.01	0.15±0.03	7.54±0.02
26.79	3.83E-08	0.108	3.263	0.925±0.003	0.26±0.01	0.13±0.01	6.92±0.04
26.12	4.77E-08	0.104	3.069	0.923±0.006	0.23±0.02	0.13±0.01	6.05±0.01
45.09	4.69E-08	0.108	5.171			0.13±0.02	
26.22		0.101	3.174	0.922±0.006	0.20±0.02	0.12±0.03	5.23±0.01
27.16	5.61E-08	0.101	3.249	0.016±0.005	0.20±0.01	0.12±0.02	4.96±0.01
26.86	5.74E-08	0.102	3.228			0.10±0.01	
27.05	5.73E-08	0.105	3.142	0.919±0.003	0.18±0.01	0.11±0.005	4.20±0.01
26.3	5.33E-08	0.105	3.055			0.10±0.01	
27.07	5.41E-08	0.103	3.126	0.919±0.003	0.17±0.01	0.11±0.005	4.15±0.01
27.39	5.60E-08	0.103	3.152			0.11±0.01	
27.16	5.26E-08	0.104	3.097	0.917±0.006	0.16±0.01	0.10±0.01	4.12±0.01
26.4	5.44E-08	0.113	3.376			0.10±0.01	
28.31	5.31E-08	0.108	3.239			0.11±0.02	
28.51	5.16E-08	0.104	3.236			0.11±0.005	
28.26	5.06E-08	0.106	3.219			0.11±0.005	
28.49	4.70E-08	0.103	3.260			0.11±0.01	
28.28	4.92E-08	0.105	3.266	0.917±0.007	0.18±0.02	0.11±0.005	4.37±0.02
28.17	5.01E-08	0.106	3.242			0.11±0.02	
				0.911±0.009	0.19±0.2		4.54±0.01
				0.924±0.006	0.16±0.01		4.22±0.01
				0.920±0.011	0.15±0.03		3.92±0.03
				0.919±0.018	0.17±0.05		4.84±0.05

throughout the soil profile. In absolute terms, the loss in remanence at low temperatures is greatest in the magnetically enhanced horizons (Fig. 2a and b), consistent with a slight increase in SP particles deduced from an increase in frequency-dependent susceptibility (Fig. 4c). In relative terms, however, the concentration of (super)paramagnetic particles remains fairly constant (Fig. 2c), which is due to the simultaneous increase of remanence carrying SD particles in the magnetically enhanced horizons and a

loss of paramagnetic minerals suggested by a decrease in χ_{hf} (Fig. 4i). Curie temperatures between 550 and 580°C (Fig. 3) suggest that a ferrimagnetic mineral close to magnetite with probably minor Ti substitution ($x < 0.1$) dominates the magnetic properties of the soil at ambient and high temperatures. Weak Verwey transitions confirm this interpretation (Fig. 2).

Increases in concentration-dependent parameters (χ , IRM) show that the A horizon is enhanced in magnetic minerals (Fig. 4a and b). The additional

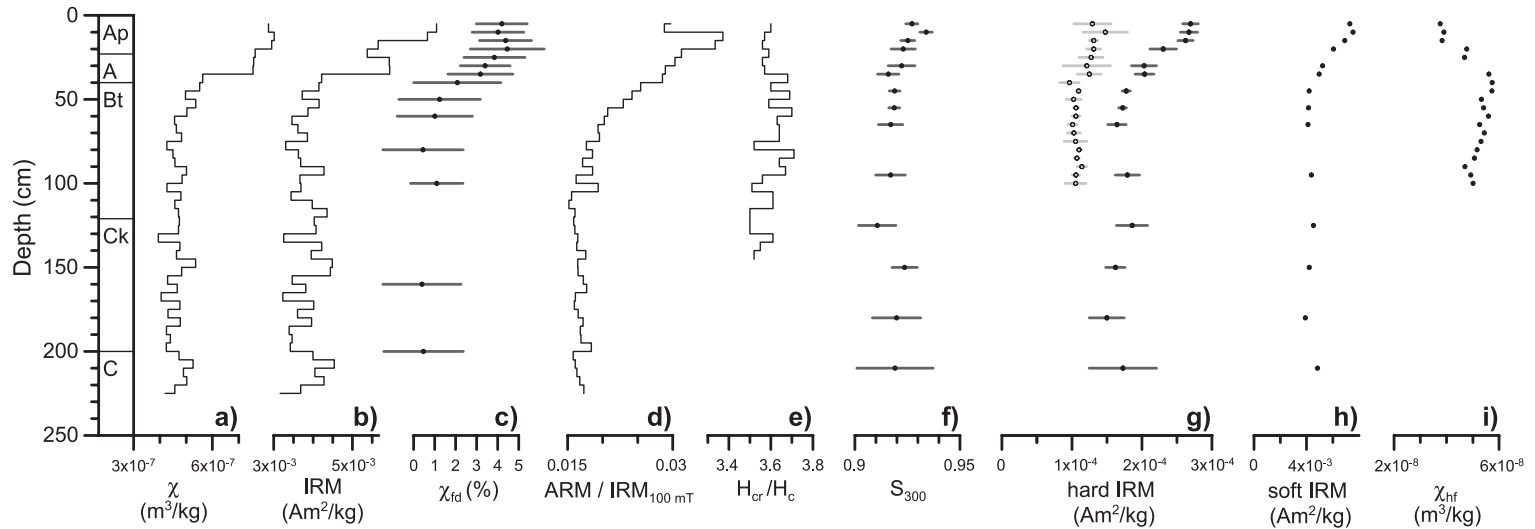


Fig. 4. Summary of magnetic properties for site 4G-99a. (a) Magnetic susceptibility (χ) and (b) isothermal remanent magnetization (IRM) are proxies for the abundance of magnetic minerals. (c) Frequency-dependent susceptibility (χ_{fd}) is a proxy for the relative abundance of ultrafine ($<0.01 \mu\text{m}$) superparamagnetic particles. (d) ARM/IRM is a proxy for the abundance of fine ($0.01\text{--}0.1 \mu\text{m}$) single-domain particles. (e) H_{cr}/H_c characterizes bulk magnetic grain size. (f) S -ratios quantify the relative abundance of low-coercivity ferrimagnetic minerals, while (g) “hard” IRM (hIRM) quantifies the absolute abundance of high-coercivity antiferromagnetic minerals, such as hematite or goethite. Solid symbols: $\text{hIRM}_{300 \text{ mT}}$, open symbols: $\text{hIRM}_{600 \text{ mT}}$. (h) “Soft” IRM (sIRM) is used to estimate the presence of low-coercivity ferrimagnetic minerals. (i) High-field susceptibility tracks the abundance of paramagnetic Fe-bearing minerals.

Table 3
Concentration of iron and selected heavy metals for selected samples from site 4G-99a

Depth (cm)	Fe ₂ O ₃ (%)	Cu (ppm)	Zn (ppm)	Pb (ppm)
15	3.01±0.05	22.18±0.44	83.22±1.87	17.80±0.42
25	3.48±0.02	24.39±0.80	89.21±2.42	18.96±0.46
45	4.15±0.05	28.50±1.16	97.36±3.10	19.44±0.65
175	3.63±0.06	26.51±0.85	92.99±1.87	17.21±0.30
220	3.68±0.08	28.97±0.89	92.91±1.44	17.47±0.14

pedogenic material is likely fine-grained (SD and smaller) leading to higher values of χ_{fd} and ARM/IRM_{100 mT} in the upper soil horizons (Fig. 4c and d). This shift to smaller, remanence carrying ferrimagnetic grains is quite small as maximum ARM/IRM_{100 mT} ratios reach only slightly above 0.03. Hysteresis parameters (only H_{cr}/H_c shown, Fig. 4e), which are a measure of the average magnetic grain size, confirm this interpretation, showing only slight changes towards finer grains in the magnetically enhanced horizon.

S-ratios between 0.9 and 0.95 (Fig. 4f) agree with the results of high- and low-temperature analyses, indicating that the magnetic component is magnetically dominated by low-coercivity (titano) magnetite or maghemite. S-ratios increase slightly in the A horizon, which suggests that pedogenetically produced magnetic signal is caused predominantly by magnetite or maghemite. The abundance of high-coercivity hematite or goethite has been estimated from hIRM measurements (Fig. 4g). hIRM increases in the upper soil horizon, which is either due to the direct generation of hematite or goethite, or the relatively rapid oxidation of pedogenic ferrimagnets (magnetite, maghemite) to antiferromagnetic minerals (hematite, goethite).

We estimated the abundance of ferri- and antiferromagnetic minerals from measurements of hIRM and sIRM. Hysteresis measurements show that all samples have ratios of $J_{rs}/J_s \approx 0.1$. Assuming that hysteresis properties are dominated by a component close to magnetite, we use a saturation remanence of $J_{mt} = 0.1 J_s \approx 0.1 \times 90 \text{ A m}^2/\text{kg}$ to estimate the amount of ferrimagnetic material based on observed values of sIRM. We further assume that the antiferromagnetic component consists of hematite or goethite with a saturation magnetization of $J_s \approx 0.1 \text{ A m}^2/\text{kg}$ [41].

Since this component is likely finer-grained, which leads to higher ratios of J_{rs}/J_s , we approximate its saturation remanence as $J_{hem} \approx 0.5 J_s = 0.05 \text{ A m}^2/\text{kg}$. Using the values for hIRM and sIRM (both measured for backfields of 300 mT) shown in Fig. 4g, we obtain concentrations ranging between 1 and 0.6 mg/cm³ for ferrimagnetic minerals and concentrations ranging between 7 and 4 mg/cm³ for antiferromagnetic minerals.

High-field susceptibility (χ_{hf}) measurements (Fig. 4i) show that the concentration of paramagnetic minerals remains relatively constant throughout the B horizon, but drops significantly for the magnetically enhanced upper part of the profile.

ICP-MS analyses of iron and heavy metal concentrations are shown in Table 3. Total iron concentrations as well as the concentrations of copper, zinc and lead all show a decrease in the magnetically enhanced soil horizons.

5. Discussion

Our study of a modern loessic soil profile from Nebraska shows a distinct magnetic enhancement in the upper soil horizon, similar to profiles in loess elsewhere in temperate regions. Preliminary, unpublished data further confirm that site 4G-99a is fairly typical for loessic soils of the midwestern United States. The magnetic enhancement is limited to the upper (Ap and A) soil horizons, though changes in grain size proxies extend farther down into the underlying Bt horizon to a maximum depth of approximately 50 cm. The added pedogenic magnetic component consists of fine-grained (SP and SD) ferri- and antiferromagnetic minerals, leading to increases in all concentration-dependent parameters (χ , ARM, IRM, J_s), as well as increases in grain-size-dependent magnetic parameters diagnostic of fine-grained magnetic material, such as χ_{fd} and ARM/IRM_{100 mT}.

Numerous coal-fired power plants exist in the western United States providing a potential source of magnetic fly-ash to our site. Site 4G-99a is approximately 100 km northeast of the nearest coal-fired power plant (Gothenburg NE) and more than 450 km downwind of the coal-fired plants located in eastern Wyoming. We did not observe any opaque spherules

in the uppermost soil horizon and concentrations of heavy metals, such as Cu, Zn or Pb do not increase towards the top of the profile, indicating the absence of significant levels of atmospheric pollution [42]. Furthermore, significant contamination of the soil profile by magnetic fly-ash seems unlikely since the magnetic enhancement is expressed in a shift towards finer SD and SP particles rather than coarse (MD) fly-ash spherules. The site has not been plowed for several decades and any recent anthropogenic contamination would be expected in the upper soil horizons, while the magnetic enhancement signal is found to a depth of approximately 40 cm.

The site is well drained and located in a stable upland position, making it ideally suited to study pedogenic effects on soil magnetic properties. The few redoximorphic features in the BC (90–120 cm) and C (>200 cm) horizons do not significantly affect the overall magnetic properties.

5.1. Mineralogy of the remanence carrying component

Even though most magnetic parameters are dominated by low-coercivity ferrimagnets (magnetite or maghemite), antiferromagnetic minerals (hematite or goethite) are the dominant remanence carrying component by mass. Our rough estimate of both components makes several assumptions regarding the grain size and resulting saturation remanence of the two components. Our assumption of an SD antiferromagnetic component with a $J_{rs}/J_r=0.5$ may underestimate its concentration. However, since hematite and goethite are likely produced in situ or during (eolian) transport, their grain size is likely rather small and below the lower grain size limit of 0.1 mm for MD-hematite [43]. We are likely to underestimate particles near the SP–SD boundary ($\approx 0.003 \mu\text{m}$ for hematite and magnetite [32]) and all (super)paramagnetic components, which might represent up to 70% of the iron-bearing fraction, based the observed loss of remanence between -275 and -200°C in low- T analyses (Fig. 2). Mössbauer analysis might allow further quantification of the ferri- and antiferromagnetic components. The identification of nanocrystalline, ionically substituted iron-components, however, is difficult and might not improve significantly our current estimates. Our simple estimates show that at

least 90% of the remanence carrying component exists in the form of hematite or goethite, rather than magnetite or maghemite.

5.2. Constraints on pathways of magnetic enhancement

Our analyses can be used to shed some light on possible pathways of magnetic enhancement. Compaction of the top soil horizons can be ruled out since the enhancement is clearly expressed in mass-normalized magnetic susceptibility and IRM, which are independent of changes in density and hence compaction. The concentration of magnetic minerals through leaching or removal of carbonates [17] is unlikely as well. Our soil descriptions show that clay increase in the Bt horizon is slight, and carbonates are leached completely from the profile to a depth of 130 cm, approximately 90 cm below the highest values of χ and IRM.

The addition of Holocene Bignell loess and hence changes in the magnetic properties of the parent material are likely to influence the studied profile to some extent. Bignell loess is not distinguished as a separate sedimentary unit in our site as pedogenesis was able to keep up with loess deposition rates, creating a welded soil profile. The good correlation of magnetic properties with soil horization, however, argues in favor of a pedogenic origin for the magnetic enhancement signal rather than a simple change in parent material.

Magnetic enhancement is also not due to conversion of weakly magnetic antiferromagnetic minerals into strongly magnetic ferrimagnetic minerals, as both increase in concentration in the upper soil horizons. It is possible, however, that paramagnetic minerals are converted into ferri- and antiferromagnetic minerals, which is suggested by the χ_{hf} distinct drop in P in the Ap and A horizons (Fig. 4i).

6. Suggestions for paleoclimate reconstructions

Many studies (e.g., [44–46]) agree that the magnetic properties of loess-paleosol sequences are dominated by coarse ferrimagnets in the PSD to MD ($>1 \mu\text{m}$) grain-size range, but that the pedogenetic magnetic component, which is responsible for the observed

magnetic enhancement, is composed of fine- to ultra-fine (<0.1 μm) magnetite or maghemite (e.g., [9,10,47,48]). Antiferromagnetic minerals, such as goethite or hematite, may comprise the bulk of the iron-bearing component of the sediment, and changes in their mineralogy may be related climatic conditions during soil formation [49], but, due to their low saturation magnetization, these minerals contribute little to the bulk magnetic signal. For these reasons, we think that the magnetic proxies most useful for transfer function between climate and magnetic soil properties should be the ones that selectively respond to this change in magnetic grain size.

Low-field magnetic susceptibility (χ), which is commonly used as a paleoprecipitation proxy, has been shown to work well in well drained, buffered and unpolluted loessic soils that contain sufficient amounts of iron to allow for the formation of pedogenic magnetic minerals (e.g., [4,18,48,50,51]). However, χ is relatively insensitive to SD particles, while it depends on a variety of other components, such as the abundance and mineralogy of paramagnetic minerals, or grain size and mineralogy changes in the parent material. For these reasons, we expect susceptibility-based paleoclimate reconstructions to perform poorly in areas like the midwestern United States, where loessic parent material is derived from different sources [52].

Enhancement parameters based on changes in ARM, ARM/IRM ratios, and frequency-dependent susceptibility (χ_{fd}) focus on this (ultra)fine-grained magnetic component and therefore offer some promise as a useful paleoprecipitation proxy. ARM, or ARM its equivalent field-normalized ARM (χ_{ARM}), has been measured for several soil sites in the United States [53], Asia [4] and on the Chinese loess plateau (e.g., [31,54]), and Liu et al. [55] use it extensively to estimate grain size variations between loess and paleosol units. Basing a paleoclimate proxy on frequency-dependent susceptibility might have several disadvantages. The SP signal derived from χ_{fd} measurements is weak and the nanocrystalline particles can be easily altered by weathering processes. Furthermore, accurate determinations of χ_{fd} are time-consuming, and the results should ideally be corrected for paramagnetic contributions. It may therefore not be feasible to apply χ_{fd} measurements to large sample sets as it will be necessary to reconstruct regional climate

change. Measurements of time-dependent IRM [56] might allow for the rapid quantification of grains near the SP–SD boundary. Time-dependent IRM is diagnostic of grain sizes slightly larger than these quantified by χ_{fd} , and both techniques yield comparable results for a wide range of well-characterized (natural and synthetic) samples. Presently, ARM or ARM/IRM might be a better foundation for paleoclimate reconstructions based on soil magnetic properties. They are easily and rapidly measured and reflect (slightly) larger SD particles, which may better withstand long-term weathering. IRM acquisition curves, S -ratios, or measurements of hIRM and sIRM may also yield useful information regarding the relative abundance and possibly mineralogy [34,57] of the high-coercivity antiferromagnetic component goethite and hematite. Combined with measurements of soil color, these magnetic parameters may yield another parameter to quantify soil moisture and temperature [49].

Acknowledgments

We would like to thank Joe Mason for his help in the field and for providing the samples and soil description for this study. Insightful reviews by B. Maher and F. Lagroix helped to enhance the quality of the manuscript. Part of the analyses were performed at the Institute for Rock Magnetism at the University of Minnesota which is funded by the W.M. Keck foundation, the National Science Foundation's Earth Science Division's Instrumentation and Facilities Program and the University of Minnesota. This is IRM publication number 0409. The study was supported by NSF grant 9909523 to SKB and CEG. During her stay at the University of Minnesota, JM was supported by an NSF REU fellowship.

References

- [1] G. Kukla, The mystery of the Chinese magnetic dust, Lamont-Doherty Geol. Obs. Yearbook, 1988.
- [2] B.A. Maher, R. Thompson, Paleorainfall reconstructions from pedogenic magnetic susceptibility variations in the Chinese loess and paleosols, *Quat. Res.* 44 (1995) 383–391.
- [3] F. Heller, C.D. Shen, J. Beer, T.S. Liu, A. Bronger, M. Suter, G. Bonani, Quantitative estimates of pedogenic ferromagnetic

- mineral formation in Chinese loess and paleoclimatic implications, *Earth Planet. Sci. Lett.* 114 (1993) 385–390.
- [4] B.A. Maher, A. Alekseev, T. Alekseeva, Variations of soil magnetism across the Russian steppe: its significance for use of soil magnetism as a paleorainfall proxy, *Quat. Sci. Rev.* 21 (2002) 1571–1576.
- [5] Y. Tang, J. Jia, X. Xie, Records of magnetic properties in Quaternary loess and its paleoclimatic significance: a brief review, *Quat. Int.* 108 (2003) 33–50.
- [6] E. Le Borgne, Influence du feu sur les propriétés magnétiques du sol et sur celles du schiste et du granite, *Ann. Geophys.* 16 (1960) 159–195.
- [7] G. Kletetschka, S.K. Banerjee, Magnetic stratigraphy of Chinese loess as a record of natural fires, *Geophys. Res. Lett.* 22 (11) (1995) 1241–1343.
- [8] H. Lu, T. Liu, Z. Gu, B. Liu, L. Zhou, J. Han, N. Wu, Effect of burning C3 and C4 plants on the magnetic susceptibility signal in soils, *Geophys. Res. Lett.* 27 (2000) 2013–2016.
- [9] X.M. Meng, E. Derbyshire, R.A. Kemp, Origin of the magnetic susceptibility signal in Chinese loess, *Quat. Sci. Rev.* 16 (1997) 833–839.
- [10] B.A. Maher, R.M. Taylor, Formation of ultrafine-grained magnetite in soils, *Nature* 336 (1988) 368–370.
- [11] D.R. Lovley, Organic matter mineralization with the reduction of ferric iron: a review, *Geomicrobiology* 5 (1987) 375–399.
- [12] F. Heller, T.S. Liu, Magnetism of Chinese loess deposits, *Geophys. J. R. Astron. Soc.* 77 (1984) 125–141.
- [13] M.J. Singer, P. Fine, Pedogenic factors affecting magnetic susceptibility of northern California soils, *Soil Sci. Soc. Am. J.* 53 (1989) 1119–1127.
- [14] X.M. Liu, P. Hesse, T. Rolph, J.E. Begét, Properties of magnetic mineralogy of Alaskan loess: evidence for pedogenesis, *Quat. Int.* 62 (1999) 93–102.
- [15] N. Bigelow, J.E. Begét, R. Powers, Latest Pleistocene increase in wind intensity recorded in eolian sediments from central Alaska, *Quat. Res.* 34 (1990) 160–168.
- [16] M.E. Evans, N.W. Rutter, N. Catto, J. Chlachula, D. Nyvlt, Magnetoclimatology: teleconnection between the Siberian loess record and North Atlantic Heinrich events, *Geology* 31 (2003) 537–540.
- [17] M.J. Singer, K.L. Verosub, P.T. Fine, J. Tenpas, A conceptual model for the enhancement of magnetic susceptibility in soils, *Quat. Int.* 34–36 (1996) 243–248.
- [18] B.A. Maher, Magnetic properties of modern soils and Quaternary loessic paleosols: paleoclimatic implications, *Palaeogeogr. Palaeoclimatol. Palaeoecol.* 137 (1998) 25–54.
- [19] B.A. Maher, R. Thompson, L.P. Zhou, Spatial and temporal reconstructions of changes in the Asian paleomonsoon: a new mineral-magnetic approach, *Earth Planet. Sci. Lett.* 125 (1994) 461–471.
- [20] B.A. Maher, H.-M. Yu, H.M. Roberts, A.G. Wintle, Holocene loess accumulation and soil development at the western edge of the Chinese Loess Plateau: implications for magnetic proxies of paleorainfall, *Quat. Sci. Rev.* 22 (2003) 445–451.
- [21] M.J. Singer, P. Fine, K.L. Verosub, O.A. Chadwick, Time dependence of magnetic susceptibility of soil chronosequences on the California coast, *Quat. Res.* 37 (1992) 323–332.
- [22] N.J. Vidic, M.J. Singer, K.L. Verosub, Duration dependence of magnetic susceptibility enhancement in the Chinese loess-paleosols of the past 620 ky, *Palaeogeogr. Palaeoclimatol. Palaeoecol.* 211 (2004) 271–288.
- [23] E.A. Oches, S.K. Banerjee, Rock-magnetic proxies of climate change from loess-paleosol sediments of the Czech Republic, *Stud. Geophys. Geod.* 40 (1996) 287–300.
- [24] J. Nawrocki, Magnetic susceptibility of Polish loesses and loess-like sediments, *Geol. Carpath.* 43 (1992) 179–180.
- [25] P.A. Vlag, P.A. Solheid, E.A. Oches, S.K. Banerjee, The paleoenvironmental-magnetic record of the Gold Hill Steps loess section in central Alaska, *Phys. Chem. Earth* 24 (1999) 779–783.
- [26] W.C. Johnson, K.L. Willey, Isotopic and rock magnetic expression of environmental change at the Pleistocene–Holocene transition in the central Great Plains, *Quat. Int.* 67 (2000) 89–106.
- [27] D.A. Grimley, L.R. Follmer, E.D. McKay, Magnetic susceptibility and mineral zonation controlled by provenance in loess along the Illinois and Central Mississippi river valleys, *Quat. Res.* 49 (1998) 24–36.
- [28] D.R. Muhs, E.A. Bettis III, J. Been, J.P. Geehin, Impact of climate and parent material on chemical weathering in loess-derived soils of the Mississippi river valley, *Soil Sci. Soc. Am. J.* 65 (2001) 1761–1777.
- [29] HPRCC, High Plains Regional Climate Center: Historical data summaries, <http://www.hprcc.unl.edu/products/historical.htm>, pp. Developed by the Western Regional Climate Center, Accessed January 16, 2004, Lincoln, NE, 2004.
- [30] C.L. Hammond, C.F. Mahnke, L. Brown, R. Schulte, W. Russell, Soil survey of Boone County, Nebraska, United States Department of Agriculture, Soil Conservation Service, Washington, DC, 1972.
- [31] C.P. Hunt, S.K. Banerjee, J. Han, P.A. Solheid, E. Oches, W. Sun, T. Liu, Rock-magnetic proxies of climate change in the loess-paleosol sequences of the western loess plateau of China, *Geophys. J. Int.* 123 (1995) 232–244.
- [32] D.J. Dunlop, Ö. Özdemir, *Rock Magnetism, Fundamentals and Frontiers*, Cambridge University Press, Cambridge, 1997 (573 pp.).
- [33] R.L. Reynolds, E. Callender, A. Goldin, J.G. Rosenbaum, P. Van Metre, M. Tuttle, Greigite (Fe₃S₄) as an indicator of drought—the 1912–1994 sediment magnetic record from White Rock Lake, Dallas, Texas, USA, *J. Paleolimnol.* 21 (1999) 193–206.
- [34] R. Egli, Characterization of individual rock magnetic components by analysis of remanence curves: 1. Unmixing natural sediments, *Stud. Geophys. Geod.* 48 (2004) 391–446.
- [35] J. King, S.K. Banerjee, J. Marvin, Ö. Özdemir, A comparison of different magnetic methods for determining the relative grain size of magnetite in natural materials: some results from lake sediments, *Earth Planet. Sci. Lett.* 59 (1982) 404–419.
- [36] C.P. Hunt, B.M. Moskowitz, S.K. Banerjee, Magnetic properties of rocks and minerals, *Rock Physics and Phase Relations*.

- A Handbook of Physical Constants, AGU Reference Shelf, vol. 3, 1995, pp. 189–204.
- [37] J. Bloemendal, J.W. King, F.R. Hall, S.-H. Doh, Rock magnetism of Late Neogene and Pleistocene deep-sea sediments: relationship to sediment source, diagenetic processes, and sediment lithology, *J. Geophys. Res.* 97 (1992) 4361–4375.
- [38] H.-U. Worm, On the superparamagnetic-stable single domain transition for magnetite, and frequency dependence of susceptibility, *Geophys. J. Int.* 133 (1998) 201–206.
- [39] R. Day, M. Fuller, V.A. Schmidt, Hysteresis properties of titanomagnetites: grain-size and compositional dependence, *Phys. Earth Planet. Inter.* 13 (1977) 260–267.
- [40] D.J. Dunlop, Hysteresis properties and their dependence on particle size: a test of pseudo-single-domain remanence models, *J. Geophys. Res.* 91 (B9) (1986) 9569–9584.
- [41] H.C. Soffel, *Paläomagnetismus und Archäomagnetismus*, Springer, Berlin, 1991, 276 pp.
- [42] J.A. Dearing, Holocene environmental change from magnetic proxies in lake sediments, in: B.A. Maher, R. Thompson (Eds.), *Quaternary Climates, Environments and Magnetism*, Cambridge University Press, Cambridge, 1999, pp. 231–278.
- [43] G. Kletetschka, P.J. Wasilewski, Grain size limit for SD hematite, *Phys. Earth Planet. Inter.* 129 (2002) 173–179.
- [44] M.E. Evans, F. Heller, Magnetic enhancement and paleoclimate: study of a loess/paleosol couplet across the loess plateau of China, *Geophys. J. Int.* 117 (1994) 257–264.
- [45] F. Florindo, R. Zhu, B. Guo, L. Yue, Y. Pan, F. Speranza, Magnetic proxy climate results from the Duanjiapo loess section, southernmost extremity of the Chinese loess plateau, *J. Geophys. Res.* 104 (1999) 645–659.
- [46] X. Li, T. Liu, M. Chen, B.A. Maher, S.K. Banerjee, Origin of magnetic minerals and magnetic susceptibility variations in Chinese loess, in: T. Liu (Ed.), *Loess Environment and Global Changes*, Science Press, China, 1991.
- [47] L.P. Zhou, F. Oldfield, A.G. Wintle, S.G. Robinson, J.T. Wang, Partly pedogenic origin of magnetic variations in Chinese loess, *Nature* 346 (1990) 737–739.
- [48] F. Heller, X. Liu, T. Liu, T. Xz, Magnetic susceptibility of loess in China, *Earth Planet. Sci. Lett.* 103 (1991) 301–310.
- [49] U. Schwertmann, Occurrence and formation of iron oxides in various pedoenvironments, in: J.W. Stucki, B.A. Goodman, U. Schwertmann (Eds.), *Iron in Soils and Clay Minerals*, Nato ASI Series, Reidel Publishing, Dordrecht, 1988, pp. 276–308.
- [50] G. Kukla, F. Heller, X.M. Liu, T.C. Xu, T.S. Liu, Z.S. An, Pleistocene climates in China dated by magnetic susceptibility, *Geology* 16 (1988) 811–814.
- [51] B.A. Maher, R. Thompson, Paleoclimatic significance of the mineral magnetic record of the Chinese loess and paleosols, *Quat. Res.* 37 (1992) 155–170.
- [52] E.A. Bettis III, D.R. Muhs, H.M. Roberts, A.G. Wintle, Last glacial loess in the conterminous USA, *Quat. Sci. Rev.* 22 (2003) 1907–1946.
- [53] Ö. Özdemir, S.K. Banerjee, A preliminary magnetic study of soil samples from west-central Minnesota, *Earth Planet. Sci. Lett.* 59 (1982) 393–403.
- [54] B.A. Maher, R. Thompson, Mineral magnetic record of the Chinese loess and paleosols, *Geology* 19 (1991) 3–6.
- [55] Q.S. Liu, S.K. Banerjee, M.J. Jackson, B.A. Maher, Y.X. Pan, R.X. Zhu, C.L. Deng, F.H. Chen, Grain sizes of susceptibility and anhysteretic remanent magnetization carriers in Chinese loess/paleosol sequences, *J. Geophys. Res.* 109 (2004) B03101.
- [56] H.U. Worm, Time dependent IRM: a new technique for magnetic granulometry, *Geophys. Res. Lett.* 26 (1999) 2557–2560.
- [57] D. Heslop, M.J. Dekkers, P.P. Kruiver, I.H.M. van Oorschot, Analysis of isothermal remanent magnetization acquisition curves using the expectation-maximization algorithm, *Geophys. J. Int.* 148 (2002) 58–64.